

Independent population coding of the past and the present in prefrontal cortex during learning

Silvia Maggi¹ and Mark D. Humphries^{1*}

1. School of Psychology, University of Nottingham, Nottingham, UK.

* Contact: mark.humphries@nottingham.ac.uk

Abstract

Medial prefrontal cortex (mPFC) plays a role in present behaviour and in short-term memory. Unknown is whether the present and the past are represented in the same mPFC neural population and, if so, how the two representations do not interfere. Analysing mPFC population activity of rats learning rules in a Y-maze, we find population activity switches from encoding the present to encoding the past of the same events after reaching the arm-end. We show the switch is driven by population activity rotating to orthogonal axes, and the population code of the present and not the past reactivates in subsequent sleep, confirming these axes were independently accessible. Our results suggest mPFC solves the interference problem by encoding the past and present on independent axes of activity in the same population, and support a model of the past and present encoding having independent functional roles, respectively contributing to on-line learning and off-line consolidation.

Keywords: decision making, mPFC, learning, neural ensembles, sleep, replay

Introduction

The medial prefrontal cortex (mPFC) plays key roles in adaptive behaviour, including reshaping behaviour in response to changes in a dynamic environment (Euston et al., 2012) and in response to errors in performance (Narayanan and Laubach, 2008; Laubach et al., 2015). Damage to mPFC prevents shifting behavioural strategies when the environment changes (Laskowski et al., 2016; Guise and Shapiro, 2017). Single neurons in mPFC shift the timing of spikes relative to hippocampal theta rhythms just before acquiring a new action-outcome rule (Benchenane et al., 2010). And multiple labs have reported that global shifts in mPFC population activity precede switching between behavioural strategies (Rich and Shapiro, 2009; Durstewitz et al., 2010; Karlsson et al., 2012; Powell and Redish, 2016) and the extinction of learnt associations (Russo et al., 2020).

Adapting behaviour depends on knowledge of both the past and the present. Deep lines of research have established that mPFC activity represents information about both. The memory of the immediate past is maintained in mPFC activity, both in tasks requiring explicit use of working memory (Baeg et al., 2003; Fujisawa et al., 2008; Spellman et al., 2015) and those that do not (Maggi et al., 2018). The use of such memory is seen in both the impairment arising from mPFC lesions (Rich and Shapiro, 2007; Young and Shapiro, 2009; Laskowski et al., 2016), and the role of mPFC in error monitoring (Laubach et al.,

33 2015). Representations of stimuli and events happening in the present have been reported
34 in a variety of decision-making tasks throughout PFC (Averbeck et al., 2006; Rigotti et al.,
35 2013; Hanks et al., 2015; Siegel et al., 2015), and specifically within rodent mPFC (Sul
36 et al., 2010; Ito et al., 2015; Guise and Shapiro, 2017).

37 Little is known though about the relationship between representations of the past and
38 present in mPFC activity. Prior studies have shown that past and upcoming choices can
39 both modulate activity of neurons in the same mPFC population (for example Baeg et al.,
40 2003; Ito et al., 2015), but none have compared the encodings of the past and present,
41 nor determined how the encoding of the present becomes the encoding of the past. Thus
42 important questions remain: how the past and present are encoded in the same mPFC
43 population, how the encoding of features in the present transforms into the encoding of
44 the past, and how that transforms solves the problem of potential interference between
45 the past and the present – that the encoding of the past does not overwrite that of the
46 present, or vice-versa, and that the two encodings can be addressed independently.

47 To address these questions, we reanalyse here mPFC population activity from rats
48 learning new rules on a Y-maze (Peyrache et al., 2009). Crucially, this task had distinct
49 trial and inter-trial interval phases, in which we could respectively examine the population
50 encoding of the present (in trials) and the past (in the intervals) of the same task features
51 or events. We first established that small mPFC populations did indeed encode both the
52 present and past of the same features of the task, respectively in the trial and in the inter-
53 trial interval. We found that these encodings were orthogonal, so that the present and the
54 past were encoded by activity evolving along independent coding axes. Crucially, we show
55 here that these encodings of the past and the present could be addressed independently:
56 population activity encoding the present was reactivated in post-training sleep, but activity
57 encoding the same features in the past was not reactivated. Moreover, the improvement
58 in the animal's performance during a session correlated with how strongly the encoding of
59 the present was reactivated. Thus, by encoding the past and present of the same events
60 on independent axes, a single mPFC population prevents interference between them, and
61 allows their independent recall.

62 Results

63 To address how the mPFC encodes the past and the present, we analyse here data from
64 rats learning rules in a Y maze, who had tetrodes implanted in mPFC before the first
65 session of training. Across sessions, animals were asked to learn one of 4 rules, which were
66 given in sequence (go to the right arm, go to the lit arm, go to the left arm, go to the
67 dark arm). Rules were switched after 10 correct choices (or 11 out of 12). There were
68 8 rule-switch sessions in total, and each animal experienced at least 2 rules. The animal
69 self-initiated each trial by running along the central stem of the Y maze and choosing
70 one of the arms (Figure 1a). The trial finished at the arm's end, and reward delivered if
71 the chosen arm matched the current rule being acquired. During the following inter-trial
72 interval the rat made a self-paced return to the start of the central arm to initiate the
73 next trial. Throughout, population activity was recorded in the prelimbic and infralimbic
74 cortex (Figure 1b), which we shall term medial prefrontal cortex (mPFC) here (Laubach
75 et al., 2018, propose that these regions are equivalent to the anterior cingulate cortex
76 in primates). This task thus allowed us to study the representation of choice and its
77 environmental context in both the present (the trial) and the immediate past (the inter-
78 trial interval).

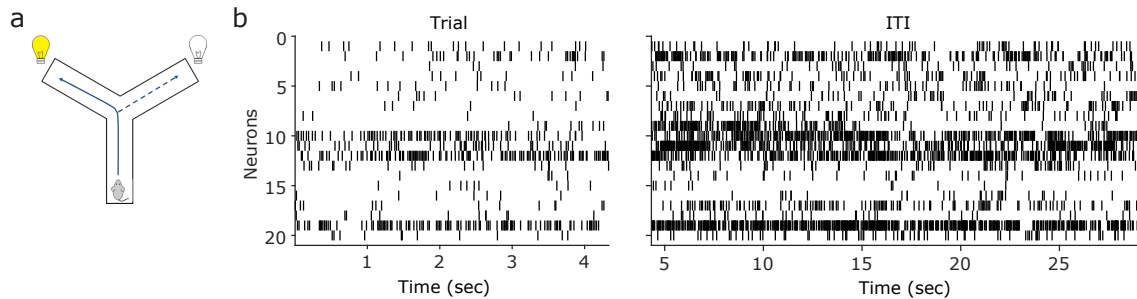


Figure 1: Task and mPFC population activity

(a) Schematic of the Y-maze task, showing a rat at the start position. A trial is the period from the start position to the end of the chosen arm; the inter-trial interval is the return from the arm end to the start position. On each trial one arm-end was lit, chosen in a pseudo-random order, irrespective of whether it was relevant to the current enforced rule. Across sessions, animals were asked to learn one of 4 rules in the sequence: go to the right arm, go to the lit arm, go to the left arm, go to the dark arm. Rules switched after 10 correct choices (or 11 out of 12). There were 8 rule-switch sessions in total, and each animal experienced at least 2 rules.

(b) Raster plots of spiking activity in the medial prefrontal cortex during a single trial and the following inter-trial interval (ITI).

79 **Population activity encodes the present and the past of the same task**
80 **features**

81 In order to compare representations of the same choice and features in the past and
82 present, we first had to establish that these were indeed represented in mPFC population
83 activity. Using a linear decoder on the vector of population activity during each trial or
84 inter-trial interval (Figure 2a), we decoded key features of the task: the animal's choice
85 of arm direction in the trial, the outcome of the trial, and which arm-end was lit during
86 the trial. Population vectors for a given session used neurons active in every trial of that
87 session, so ranged from 4-22 neurons across 49 sessions, of between 7-51 trials each (Figure
88 2 – SI Figure 1). We trained the same decoders using the same population vectors but
89 with features shuffled across trials (see Methods), to define appropriate chance levels for
90 each decoder given the unbalanced distribution of some task features, such as outcome.

Figure 2: Pfc population encoding of the past and present of the same task features

(a) Schematic of a linear decoder of population activity during a session's trials. Trials were repeatedly divided into a training set and one held-out test trial. The population vector of neuron firing rates for each trial in the training set (shade of blue squares) is input to a linear decoder that fits the weight (shade of yellow squares) for each neuron across the trials. A linear combination of the learnt weight vector and the firing rate vector of the trials is compared to a threshold (red dashed line) to predict the category to which that trial belongs. Decoding accuracy is the proportion of correctly predicted held-out trials when using the weight vector from their corresponding training set trials.

(b) Decoding accuracy for population activity during the trials of each session. In black we plot the accuracy of decoding the choice of arm direction (Dir), light position (Lig), and outcome (Out) for the current trial (left panel), and the previous trial (right panel). In grey we plot the decoding accuracy of shuffled labels across trials. Significant data decoding was tested using paired Wilcoxon signed rank test: * $p < 0.05$; ** $p < 0.01$; *** $p < 0.001$. Symbols plot means \pm SEM across 49 sessions.

(c) as for panel (b), but for population activity during the inter-trial intervals (ITI) of each session.

(d)–(e) as for panels (b)–(c), but using each session's relative decoding accuracy: the difference between the decoding accuracy of the data and of the mean of the shuffled data in that session. Here and all further panels, P-values are given for a Wilcoxon signed rank test against zero median.

(f) Breakdown of the trial decoding results in panel (d) by the rule type of each session (15 direction rule sessions; 34 cue rule sessions).

(g) As for panel (f), breakdown of the inter-trial interval decoding results by the rule-type of each session.

(h) Breakdown of the trial decoding results in panel (d) by whether a rule was learnt in a session or not (10 identified learning sessions; 39 other sessions).

(i) As for panel (h), breakdown of the inter-trial interval decoding results by learning and other sessions.

92

93 We could decode all of direction choice, outcome, and light position in the current
94 trial above chance (Figure 2b,d, left). In Figure 2b we plot the absolute accuracy of
95 decoding, to show that the decoding could be near-perfect; in Figure 2d we also plot the
96 decoding accuracy relative to the shuffled data for each session, which, as it accounts for
97 the different distributions of features (e.g. outcome) in each session, better shows the
98 effect size of the decoding. To test for effects of task history on population activity, we
99 also decoded the direction choice, outcome, and light position of the preceding trial, and
100 found that decoding was at or close to chance (Figure 2b,d, right).

101 By contrast, from population activity during the inter-trial interval we could decode
102 the direction choice, outcome, and light position of the immediately preceding trial well
103 above chance (Figure 2c,e, right). Decoding the same feature of the immediately following
104 trial was at chance (Figure 2c,e, left). Thus, the present and the past of key features of a
105 trial could both be decoded from mPfc population activity: the present direction choice,
106 outcome, and light position during the trial, and the past direction choice, outcome, and
107 light position during the inter-trial interval.

108 We explored the extent to which this decoding of the present in trials and of the past in
109 the inter-trial intervals depended on what occurred during each session. We first split the
110 sessions by whether the target rule was direction-based (15 sessions), and thus egocentric,
111 or cue-based (34 sessions) and thus allocentric. For trials, the present direction choice and
112 outcome could still be significantly decoded for both types of rule, despite the considerable
113 drop in power from 49 to 15 and 34 sessions (Figure 2f). For inter-trial intervals, the
114 preceding direction choice, outcome, and light position could still be decoded well above
115 chance for both types of rule (Figure 2g).

116 In order to determine if learning itself affected any mPfc representations of the present,

117 we then separated the sessions into two behavioural groups: putative learning sessions
118 ($n = 10$), identified by a step-change in task performance (Figure 2 – Supplementary
119 Figure 2), and the remaining sessions, called here “Other” ($n = 39$). We found decoding
120 of task features was similar when comparing learning sessions and all Other sessions for
121 both trials (Figure 2h) and inter-trial intervals (Figure 2i). The sole exception, of decoding
122 the current light position during trials of Other sessions but not learning sessions, could
123 be due either to a real effect, or to the low power for decoding from 10 learning sessions.

124 It is likely that the mPFC encoding of task features is partly dependent on maze position
125 (Ito et al., 2015; Spellman et al., 2015). To further examine the evolution of encoding over
126 the trial and inter-trial interval, we divided the maze into five equally sized sections, and
127 constructed population firing rate vectors for each position (Figure 2 – Supplementary
128 Figure 3). Even though the trials averaged only 4 seconds in duration, and so each
129 position was occupied for one second or less, we still obtained clear evidence for decoding
130 the current trial’s direction choice, outcome, and light position across multiple contiguous
131 locations. The contrast between the strong encoding of the current trial’s features and
132 the weak encoding of the previous trial’s features was even clearer across maze positions.
133 Figure 2–Supplementary Figure 4 confirms that these results are robust to breaking down
134 the position decoding by the type of rule or by learning behaviour. Crucially, no matter
135 how we examined the decoding by position, it showed that the population encoding is
136 contiguous from the trial to the following inter-trial interval for all three features (see esp.
137 Figure 2 – Supplementary Figure 3b): the encoding of the present in the trial at the arm
138 end is immediately transformed into the encoding of the past in the inter-trial interval.

139 **Independent encoding of the past and the present**

140 Having established evidence that a single mPFC population encodes both the present and
141 the past of the same features of a rule-learning task, we could now address the key question
142 of the relationship between these representations. In particular, we sought to address how
143 encoding of features in the present transforms into the encoding of the past, and if this
144 is done in a way to minimise interference between them, such that the representations of
145 the past and present can be independently accessed and activated.

146 One hypothesis is that there is no transformation: that sustained activity in mPFC
147 continues from the trial into the inter-trial interval, creating a memory trace of the encod-
148 ing during the trial. Another plausible hypothesis is that the population activity in the
149 trial reactivates during the inter-trial interval, in some form of replay of waking activity.
150 Both hypotheses predict that the population encoding of a feature in the trial and in the
151 following inter-trial interval should be the same. We show here it is not.

152 One simple way to rule out the memory trace and reactivation hypotheses would be
153 if the active neurons during the trial and inter-trial interval were different. However, the
154 active neurons during the trials were also active during the inter-trial interval (Figure 2 -
155 Supplemental Figure 1c), so this shared common population could, in principle, carry on
156 encoding the same task features.

157 We used this common population to test whether mPFC populations were encoding
158 the past and the present in the same way: if the encoding was broadly the same, then
159 the activity in the trial and following inter-trial interval should be interchangeable when
160 predicting the same feature, such as the chosen direction. In this cross-decoding test (Fig-
161 ure 3a), we first trained a linear decoder for features of the present using the common
162 population’s activity during the trials, and then tested the accuracy of the linear decoder
163 when using the common population’s activity during the inter-trial interval. If the popu-
164 lation encoding in the trials was re-used in the inter-trial interval, then this cross-decoding

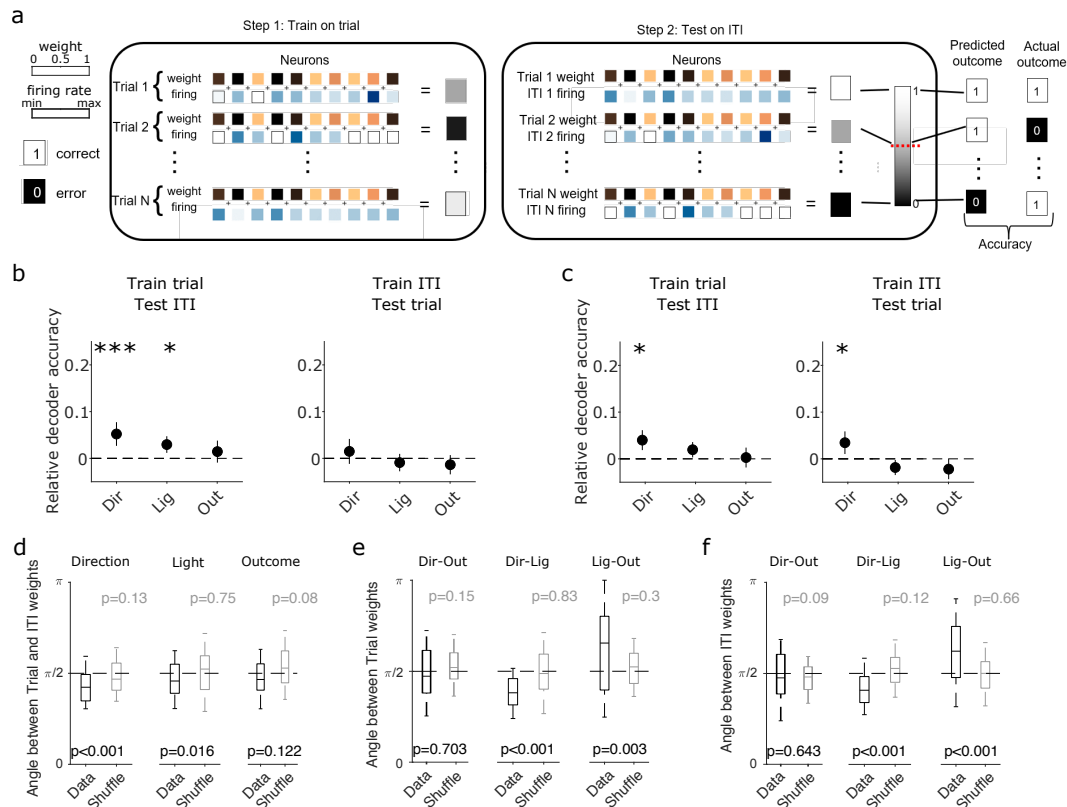


Figure 3: Independent population encoding of past and present task events.

(a) Schematic of cross-decoding the same task feature. We train the decoder of a feature using the activity in the trials of a session, then test the accuracy of decoding the same feature (now in the past) from the activity in the inter-trial intervals. (Or vice-versa: training the decoder on the inter-trial intervals (ITIs), and testing the decoding accuracy on the trials). We did this in two ways. First, as per Figure 2, we used leave-one-out cross validation, by leaving out the i th trial-ITI pair, training on $N - 1$ trials, and predicting the i th ITI. Second we used full cross-decoding, training the decoder on all N trials to get one weight vector for the decoder, and testing the decoding accuracy on all ITIs using that vector (and vice-versa).

(b) Cross-decoding performance for each task feature of the current trial, using leave-one-out cross-validation. Left: performance when the decoder was trained on activity during trials and tested on activity in the inter-trial intervals. Black dashed line shows the chance levels obtained training the classifier on shuffled labels for the trials and testing on inter-trial intervals given the same shuffled labels. Right: performance when the decoder was trained on activity from the inter-trial intervals, and tested on activity in the trials.

(c) As per (b), cross-decoding performance of the same task feature, using full cross-decoding.

(d) Comparison of the decoding vector weights between trials and inter-trial intervals. For each session we plot the angle between its trial and inter-trial interval decoding weight vectors, obtained from the trained decoders in panel (c). For reference, we also compute the angle between trial and inter-trial interval decoding vectors obtained by training on shuffled label data (grey). Boxplots show median (line), inter-quartile range (box), and 95% interval (tails). P-values are from Wilcoxon ranksum tests for the difference from $\pi/2$.

(e) As for (d), but comparing the decoding weight vectors between features, within trials.

(f) As for (e), for within inter-trial intervals.

165 should be accurate.

166 We found that cross-decoding of features was consistently poor, whether we trained on
167 trial activity and tested on inter-trial intervals, or vice-versa (Figure 3b). Decoding of all

168 features was at or close to chance, strikingly at odds with the within-trial (Figure 2b,d) or
169 within-interval (Figure 2c,e) decoding. This poor cross-decoding was robust to whether
170 we used leave-one-out cross-validation (Figure 3b), or trained the decoder on every trial
171 or every inter-trial interval (Figure 3c). We also found consistently poor cross-decoding of
172 all features when we tested at different positions along the maze (Figure 3 – Supplemental
173 Figure 1). These results suggest that population encoding of prior events in the inter-trial
174 interval is not simply a memory trace or reactivation of similar activity in the trial. Instead,
175 they show that the same mPFC population is separately and independently encoding the
176 present and past of the same features.

177 To quantify this independence, we turned to the vector of decoding weights for the
178 trials and the equivalent vector for the inter-trial intervals of the same session. These
179 weights, obtained from the decoder trained once on all trials and then once on all inter-trial
180 intervals, give the relative contribution of each neuron to the encoding of task features. We
181 found that the trial and inter-trial interval weight vectors were approximately orthogonal
182 for all three features: the angles cluster at or close to $\pi/2$ (or, equivalently, their dot-
183 product clusters at or around zero) (Fig 3d). Median angles for direction choice and light
184 position were significantly less than $\pi/2$ (ranksum test), but the difference was small:
185 0.067π for direction and 0.045π for light position. Thus, the population encoding in the
186 inter-trial interval was not a memory trace: to a good approximation, the past and present
187 are orthogonally encoded in the same mPFC population.

188 We considered a range of alternative explanations for these results. One is that the or-
189 thogonality arises from the curse of dimensionality: the distance between two i.i.d random
190 vectors with a mean of zero tends to grow with their increasing dimension. If the decoding
191 weights were random vectors, then the apparent orthogonality could be driven by just the
192 largest mPFC populations. However, the decoding weights for the whole trial (present)
193 or whole inter-trial interval (past) are not random vectors, for if they were then decoding
194 performance would be at chance, whereas we find clear decoding of all features (Figure
195 2b-e). Another explanation is that the independent encoding axes between the trials and
196 inter-trial intervals is somehow driven by differing properties of the trials and inter-trial
197 intervals. For example, they differ in duration (mean 6.5 ± 0.01 seconds for trials, 55.7
198 ± 0.03 seconds for inter-trial intervals), and hence also in average movement speed. If
199 switching between trials and inter-trial intervals could account for encoding differences,
200 then these differences should be symmetric: we should see encodings change whether the
201 transition was from the trial to inter-trial interval, or from the inter-trial interval back
202 to a trial. However, the encodings were asymmetric: we saw strong encoding during the
203 transition from trial to inter-trial interval (Figure 2b-c and Figure 2 – Supplementary
204 Figure 3), but no encoding during the transition from inter-trial interval back to the trial
205 (Figure 2b-c and Figure 2 – Supplementary Figure 3; and see Maggi et al. (2018)). In the
206 absence of any encoding, there cannot be an orthogonal shift in encoding.

207 To understand how the independent encoding between past and present related to how
208 the features were jointly encoded in the population activity, we examined the relationship
209 between the features' encoding vectors during the trial and during the inter-trial interval.
210 The encoding axes within an epoch were less independent than between epochs: angles
211 between the encoding vectors for light and direction and for light and outcome were
212 significantly different from $\pi/2$ (Figure 3e,f). But the distributions of angles between
213 the encoding vectors were preserved between the trials and the inter-trial intervals, with
214 outcome-direction around $\pi/2$, light-direction centered below $\pi/2$, and light-outcome cen-
215 tred above $\pi/2$. Thus, while each encoding axis rotated to an orthogonal direction between
216 the trial and inter-trial interval, the internal relationships between the feature encodings

217 was preserved.

218 Population activity rotates between trials and inter-trial intervals

219 That all three feature encodings were independent between the trials and inter-trial inter-
220 vals of a session predicts that the population activity itself should be independent between
221 the two. If true, then trial and inter-trial interval population activity vectors should be
222 easily separable. To test this prediction, we projected all population activity vectors of a
223 session (Fig 4a) into a low dimensional space (Fig 4b), and then quantified how easily
224 we could separate them into trials and inter-trial intervals. Using just one dimension was
225 sufficient for near-perfect separation in many sessions; using two was sufficient for above-
226 chance performance in all sessions (Fig 4c; and see Figure 4 – Supplementary Figure 1 for
227 a breakdown of each session’s dependence on the number dimensions). Population activity
228 was thus about as independent between the trials and inter-trial intervals as it possibly
229 could be.

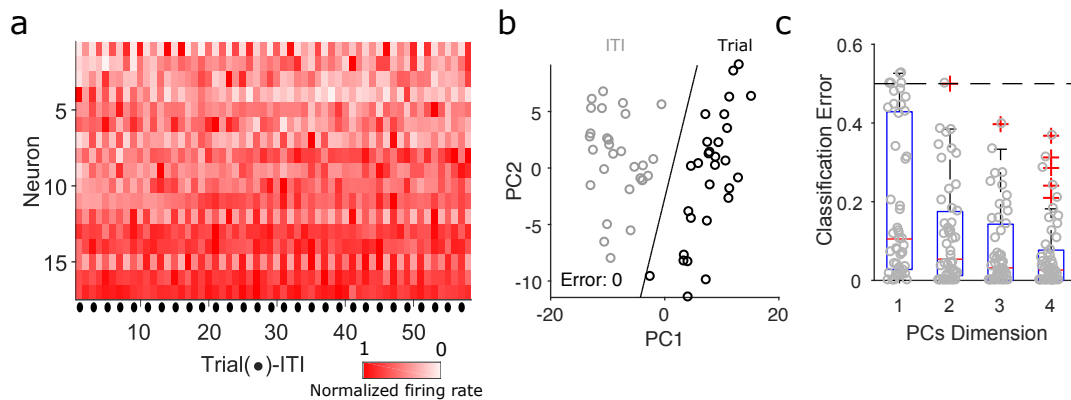


Figure 4: Population activity is independent between trials and inter-trial intervals

(a) Population activity vectors for the trials (●) and following inter-trial intervals of one session. The heat-map shows the normalized firing rate for each neuron.

(b) Projection of that session’s population activity vectors on to two dimensions shows a complete separation of trial and inter-trial interval activity. The black line is the linear separation found by the classifier. PC: principal component.

(c) Summary of classification error over all sessions, as a function of the number of dimensions. Each grey dot is the error for one session at that number of projecting dimensions. Dashed line gives chance performance. Boxplots show medians (red line), interquartile ranges (blue box), and outliers (red pluses).

230 The independence in the population activity might arise from the continuous evolution
231 of mPFC population activity across the contiguous trial and inter-trial interval period, such
232 as the sequential activation of PFC neurons observed in previous studies (e.g. Fujisawa
233 et al., 2008). If sequential activation was ongoing, then we should also observe consistently
234 independent population activity between consecutive sections of the maze during trials and
235 during inter-trial intervals. Instead, we found population activity was not independent
236 between contiguous maze sections within trials or within inter-trial intervals (Figure 4 –
237 Supplementary Figure 2a-c). Across the whole maze, population vectors from adjacent
238 sections within trials and inter-trial intervals had classification errors consistently greater
239 than any found between trials and inter-trial intervals (Figure 4 – Supplementary Figure
240 2), even when the animal was in the same maze position. Thus, while population activity
241 evolved during the trial and during the inter-trial interval, corresponding to the evolution
242 of feature encoding across the maze (Figure 2 – Supplementary Figure 3), this evolution

243 happened along independent directions in the trials and in the inter-trial intervals.

244 **Population representations of trial features re-activate in sleep**

245 Encoding the past and present of the same features in the same population faces the
246 problem of interference: of how a downstream read-out of the population's activity knows
247 whether it is reading out the past or the present. Our finding that the encoding is on
248 independent axes means that, in principle, the representations of past and present can be
249 addressed or recalled independently, without interfering with each other. We thus sought
250 further evidence of this independent encoding by asking if either representation could be
251 recalled independently of the other.

252 Prior reports showed that patterns of mPFC population activity during training are
253 preferentially repeated in post-training slow-wave sleep (Euston et al., 2007; Peyrache
254 et al., 2009; Singh et al., 2019), consistent with a role in memory consolidation. However,
255 it is unknown what features these repeated patterns encode, and whether they encode
256 the past or the present or both. Thus, we took advantage of the fact that our mPFC
257 populations were also recorded during both pre- and post-training sleep to ask which, if
258 any, of the trial and inter-trial interval codes are reactivated in sleep, and thus whether
259 they were recalled independently of each other.

260 We first tested whether population activity representations in trials reactivated more
261 in post-training than pre-training sleep. For each feature of the task happening in the
262 present (e.g. choosing the left arm), we followed the decoding results by creating a popu-
263 lation vector of the activity specific to that feature during a session's trials. To seek their
264 appearance in slow-wave sleep, we computed population firing rate vectors in pre- and
265 post-training slow-wave sleep in time bins of 1 second duration, and correlated each sleep
266 vector with the feature-specific trial vector (Figure 5a). We thus obtained a distribution
267 of correlations between the trial-vector and all pre-training sleep vectors, and a similar
268 distribution between the trial-vector and all post-training sleep vectors. Greater correla-
269 tion with post-training sleep activity would then be evidence of preferential reactivation
270 of feature-specific activity in post-training sleep.

271 We examined reactivation separately between learning and Other sessions, seeking
272 consistency with previous reports that reactivation of waking population activity in mPFC
273 most clearly occurs immediately after rule acquisition (Peyrache et al., 2009; Singh et al.,
274 2019). Figure 5b (upper panels) shows a clear example of a learning session with prefer-
275 ential reactivation. For all trial features, the distribution of correlations between the trial
276 and post-training sleep population activity is right-shifted from the distribution for pre-
277 training sleep. For example, the population activity vector for choosing the right arm is
278 more correlated with activity vectors in post-training (Post-R) than pre-training (Pre-R)
279 sleep.

280 Such post-training reactivation was not inevitable. In Figure 5b (lower panels), we
281 plot another example in which the trial-activity vector equally correlates with population
282 activity in pre- and post-training sleep. Even though specific pairs of features (such as the
283 left and right light positions) differed in their overall correlation between sleep and trial
284 activity, no feature shows preferential reactivation in post-training sleep.

285 These examples were recapitulated across the data (Figure 5c). In learning sessions,
286 feature-specific activity vectors were consistently more correlated with activity in post-
287 than pre-training sleep. By contrast, the Other sessions showed no consistent preferential
288 reactivation of any feature vector in post-training sleep. As a control for statistical arte-
289 facts in our reactivation analysis, we looked for differences in reactivation between paired
290 features (e.g. left versus right arm choice) within the same sleep epoch and found these

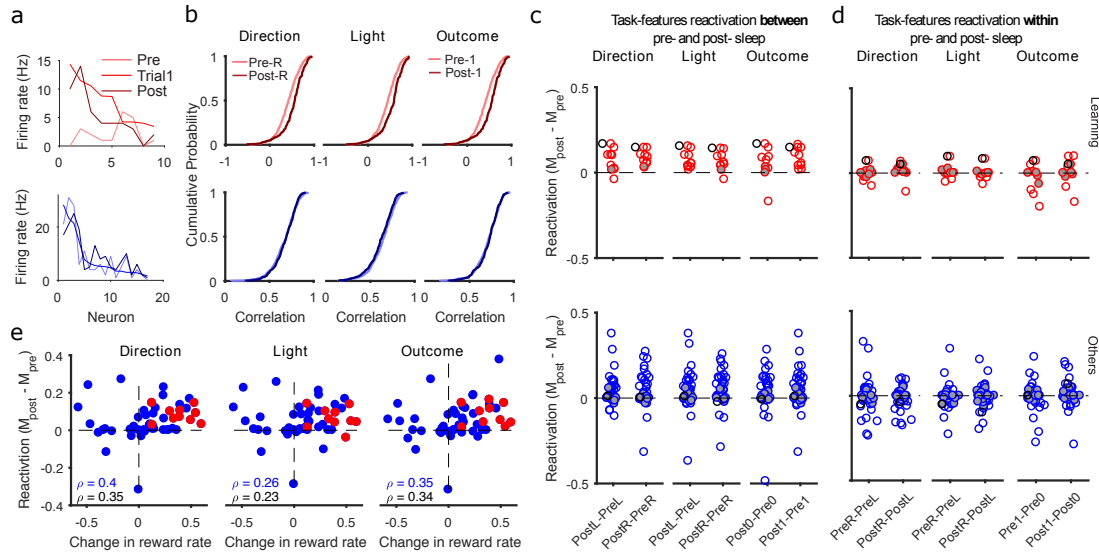


Figure 5: Reactivation of trial population coding in post-training sleep.

(a) Example population activity vectors. Upper panel: from one learning session, we plot the average firing rate vector for correct trials (Trial1). For comparison, we also plot examples of firing rate vectors from pre- and post-training slow-wave sleep (1s bins). Neurons are ranked in order of their firing rates in the trial vector. Lower panel: as for the upper panel, for an example session not classified as learning.

(b) Example distributions of Spearman's rank correlations between trial and sleep population activity. Upper panels: for the same learning session as panel (a), we plot the distributions of correlations between each vector of feature-specific trial activity and the population activity vectors in pre- and post-training slow-wave sleep. Lower panels: as for the upper panels, for the example non-learning session in panel (a). R: right arm; 1: rewarded trial.

(c) Summary of reactivations across all sessions. For each feature, we plot the difference between the medians of the pre- and post-training correlation distributions. A difference greater than zero indicates greater correlation between trials and post-training sleep. Each symbol is a session. Empty symbols are sessions with significantly different correlation distributions at $p < 0.05$ (Kolmogorov-Smirnov test). Grey filled symbols are not significantly different. One black circle for learning and one for non-learning sessions identify the two example sessions in panels (a) and (b).

(d) As for panel c, but plotting the median differences between distributions for paired features within the same sleep epoch. For example, in the left-most column, we plot the difference between the correlations with pre-session sleep activity for right-choice and left-choice specific trial vectors (PreR - PreL).

(e) Reactivation as a function of the change in reward rate in a session. One symbol per session: learning (red); Other (blue). ρ : Spearman's correlation coefficient. Black ρ is for all 49 sessions; blue ρ , using only sessions with any incremental improvement in performance ($N = 33$ in total, 10 learning and 23 Other sessions; see Methods). We plot here reactivation of vectors corresponding to left (direction and light) or correct; correlations for other vectors are similar in magnitude: 0.37 (choose right), 0.35 (cue on right), 0.2 (error trials) for all 49 sessions; 0.37 (choose left), 0.33 (cue on right) and 0.26 (error trials) for sessions with incremental improvement in performance.

291 all centre on zero (Figure 5d). Thus, population representations of task features in the
 292 present were reactivated in sleep, and this consistently occurred after a learning session.

293 To check whether reactivation was unique to step-like learning, we turned to the Other
 294 sessions: there we found a wide distribution of preferential reactivation, from many about
 295 zero to a few reactivated nearly as strongly as in the learning sessions (Figure 5c, blue

296 symbols). Indeed, when pooled with the learning sessions, we found reactivation of a
 297 feature vector in post-training sleep was correlated with the increase in accumulated reward
 298 during the session's trials (Fig 5e). Consequently, reactivation of population encoding
 299 during sleep may be directly linked to the preceding improvement in performance.

300 Prior reports suggest that the reactivation of activity patterns in sleep can be faster
 301 or slower during sleep than they were during waking activity. We tested the time-scale
 302 dependence of feature-vector reactivation by varying the size of the bins used to create
 303 population vectors in sleep, with larger bins corresponding to slower reactivation. We
 304 found that preferential reactivation in post-training sleep in learning and (some) Other
 305 sessions was robust over orders of magnitude of vector widths (Figure 6a). Notably, in
 306 the learning sessions only the vectors for rewarded outcome were significantly reactivated.
 307 Moreover, among Other sessions, the reactivation in post-training sleep was significant
 308 only for those sessions in which the animal's performance improved (however slightly)
 309 within the session (Figure 6b). This consistency across broad time-scales suggests that
 310 it is the changes during trials to the relative excitability of neurons within the mPFC
 311 population that are carried forward into sleep (Singh et al., 2019). Thus, this consistency
 312 across broad time-scales implies that whenever the encoding neurons are active, they are
 313 active together with approximately the same ordering of firing rates.

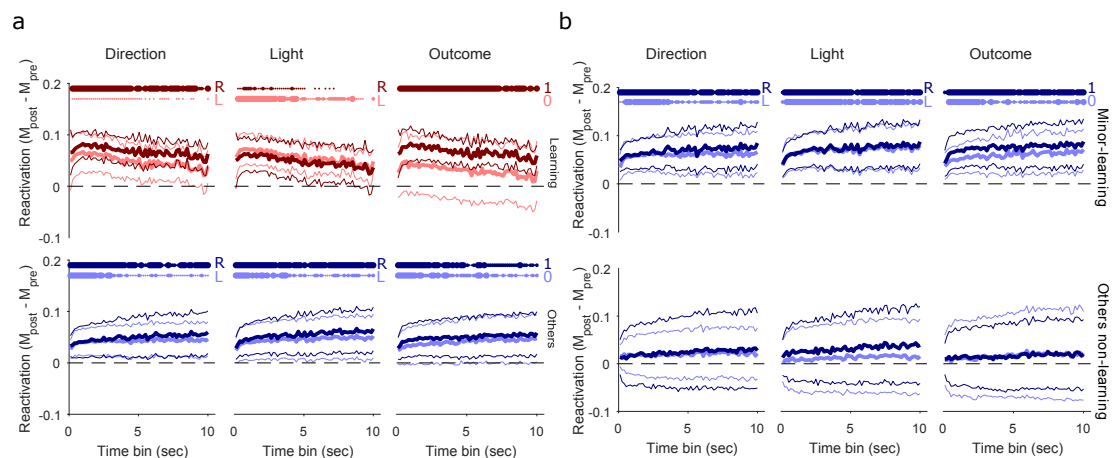


Figure 6: Robust reactivation of trial population coding across time-scales of sleep activity.

(a) At each time bin used to construct population activity vectors in sleep, we plot the distribution over sessions of the median differences between pre- and post-training correlation distributions, for learning (top), and other (bottom) sessions. Distributions are plotted as the mean (thick lines) \pm 2 SEM (thin lines); at the 1s bin, these summarise the distributions shown in full in Figure 5c. Each panel plots two distributions, one per pair of features: lighter colours indicate left or error trials (L or 0); while darker colours indicate right or correct trials (R or 1). Time bins range from 100 ms to 10 s, tested every 150 ms. Dotted lines at the top of each panel indicate bins with reactivation significantly above zero (Wilcoxon sign rank test, $p < 0.05$ thin dot; $p < 0.01$ middle size dot; $p < 0.005$ thicker dots; $N = 10$ learning, $N = 39$ Other sessions).

(b) Here we divide the Other sessions from panel (a) into those showing any increment in performance from the animal ($N = 23$, “Minor-learning”, see Methods) and those that did not ($N = 16$).

314 No re-activation in sleep of inter-trial interval feature representations

315 To ask if this reactivation was unique to encoding of the present, we repeated the same
 316 reactivation analysis for population vectors from the inter-trial interval. Again, following

317 our decoding results, each population feature vector was created from the average activity
318 during inter-trial intervals after that feature (e.g. choose left) had occurred. We then
319 checked for reactivation of this feature vector in pre- and post-training slow-wave sleep.

320 We found absent or weak preferential reactivation of population encoding in post-
321 training sleep, for any feature in any type of session (Figure 7a). Consistent with this, we
322 found no correlation between the change in performance during a session and the reactivation
323 of feature vectors after a session (Figure 7b). The orthogonal population encoding
324 during sessions (Figure 3) thus appears functional: population encoding of features in the
325 present was reactivated in sleep, but encoding of the same features in the past was not.

326 Discussion

327 We have shown that medial PFC population activity independently represents the past
328 and present of the same task features. First, we showed that the same task feature, such
329 as the choice of arm, is encoded by the same population in both the trials and the inter-
330 trial intervals, as respectively the present and past of that feature. Second, vectors of
331 population activity were about as independent between the trials and following inter-trial
332 intervals as they could possibly be. Consequently, within mPFC populations, the past and
333 the present of each feature were encoded on independent axes. Finally, we showed that
334 these independent axes indeed allow the past and present encodings to be independently
335 addressed: population activity representations of features during the trials are re-activated
336 in post-training sleep, but inter-trial interval representations are not.

337 Mixed population coding in mPFC

338 Consistent with prior reports of mixed or multiplexed coding by single neurons in the pre-
339 frontal cortex (Jung et al., 1998; Horst and Laubach, 2012; Rigotti et al., 2013; Fusi et al.,
340 2016; Aoi et al., 2020), we found that small mPFC populations can sustain mixed encoding
341 of two or more of the current trial's direction choice, light position, and outcome. These
342 encodings were also position-dependent. Encoding of direction choice reliably occurred
343 from the maze's choice point onwards, but it is unclear whether this represents a causal
344 role in the choice itself, or an ongoing representation of a choice being made.

345 Previous studies have reported encoding of past choices in mPFC population activity
346 during trials (Baeg et al., 2003; Sul et al., 2010). In contrast to the robust encoding
347 of the present, we found weak evidence that mPFC activity during a trial encoded the
348 light position of the previous trial, and weak evidence that it encoded the previous trial's
349 direction choice only during direction-based rules (and note that knowledge of the previous
350 trial's choice was not required for the direction rules). Moreover, we showed these could
351 only be decoded at one or two locations on the maze. Thus, during trials population
352 activity in the prefrontal cortex had robust, sustained encoding of multiple events of the
353 present, but at best weakly and transiently encoded one event of the past.

354 We also report that these mixed encodings of the present within each population
355 reactivate in post-training sleep. This finding goes beyond prior reports that specific
356 patterns of trial activity reactivate in sleep (Euston et al., 2007; Peyrache et al., 2009;
357 Singh et al., 2019) to show what those patterns were encoding – multiple features of the
358 present, but not the past. It seems mixed encoding is a feature of sleep too.

359 As we showed in (Maggi et al., 2018) and extended here, population activity during the
360 inter-trial interval also has mixed encoding of features of the past. Collectively, our results
361 show that population activity in mPFC can switch from mixed encoding of the present in

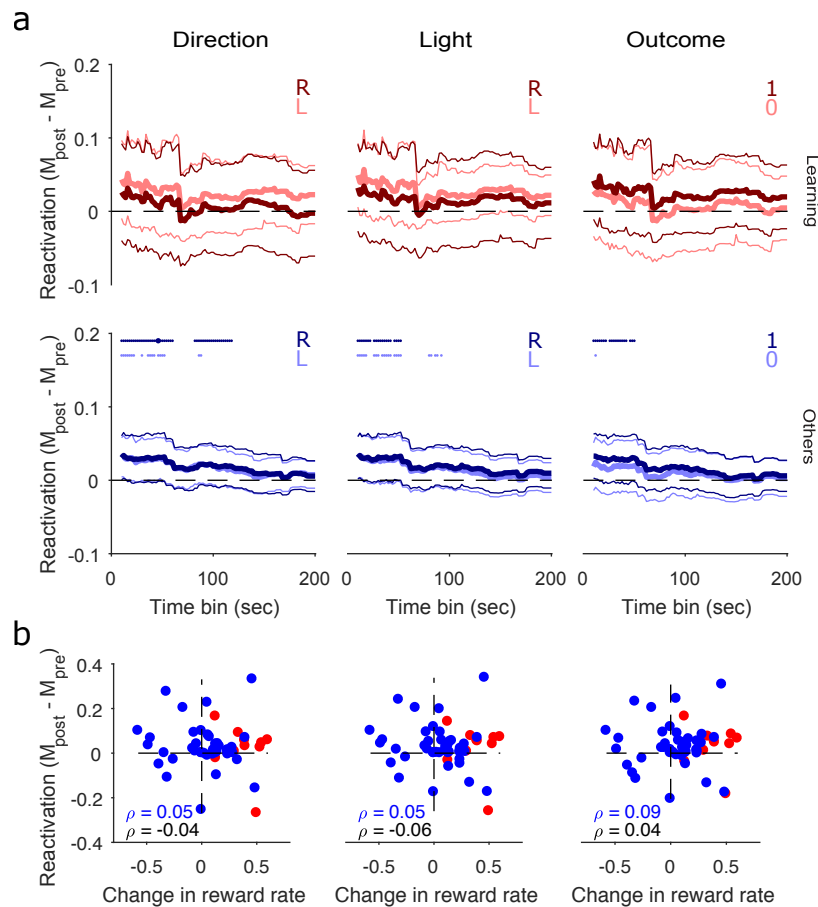


Figure 7: No consistent reactivation of population encoding of the past.

(a) Similar to Figure 6, for reactivation of population feature-vectors constructed from inter-trial interval activity. We plot the distribution over sessions of the median differences between pre- and post-training correlation distributions, for learning (top), and Other (bottom) sessions. Note that the range of sleep vector time-bins is an order of magnitude larger than for trials, as the inter-trial intervals themselves are an order of magnitude longer than trials. Dotted lines at the top indicate significant reactivation (Wilcoxon sign rank test, $p < 0.05$ thin dot; $p < 0.01$ middle size dot; $p < 0.005$ thicker dots). Lighter colours indicate left or error trials (L or 0); while darker colours indicate right or correct trials (R or 1)

(b) Similar to Figure 5e, reactivation of the inter-trial interval population vector as a function of the change in reward rate in a session. Reactivation is computed for 22 s bins. One symbol per session: learning (red); Other (blue). ρ : Spearman's correlation coefficient; black, all sessions; blue, only sessions with any incremental improvement in performance. We plot here reactivation of vectors corresponding to left (direction and light) or correct trials; correlations for other vectors are similar in magnitude: -0.004 (choose right), 0.02 (cue on right), -0.08 (error trials) for all sessions; -0.005 (choose right), 0.01 (cue on right) and -0.1 (error trials) for sessions with incremental improvement in performance.

362 a trial to mixed encoding of the past in the following inter-trial interval.

363 Independent population codes solve interference of past and present

364 There are multiple hypotheses for how this transition from coding the present to the past
 365 could happen. One hypothesis is that there are groups of neurons separately dedicated
 366 to encoding the past and present. We ruled out this idea by only decoding from neurons
 367 active in every trial and inter-trial interval, so showing that the transition from present to

368 past happened within the same group.

369 Another hypothesis, as we noted in the Results, is that the switching from a population
370 encoding of the present to encoding of the past is explained by population activity in the
371 trials being carried forward into the inter-trial interval, whether by persistent activity
372 acting as a memory trace, or by the recall of patterns of trial activity during the inter-trial
373 interval. But our demonstration of independent encoding in the population between trials
374 and the following inter-trial intervals rules out this hypothesis.

375 Our results support dynamic coding in mPFC: population encoding evolved within
376 both the trials and the inter-trial intervals, consistent with the underlying changes we
377 observed in the population activity. The evolution of population dynamics over the inter-
378 trial interval is consistent with reports of dynamic changes of PFC activity during the
379 delay period of working memory tasks in primates (Murray et al., 2017; Spaak et al.,
380 2017; Wasmuht et al., 2018), including in primate anterior cingulate cortex (Cavanagh
381 et al., 2018), a potential homologue of the medial prefrontal cortex in rodents (Laubach
382 et al., 2018). The evolving coding we observed thus supports the hypothesis that working
383 memory is sustained by population activity rather than the persistent activity of single
384 neurons (Constantinidis et al., 2018; Lundqvist et al., 2018). Crucially, the evolution of
385 activity within trials and inter-trial intervals was continuous, with adjacent maze sections
386 containing more similar population activity, yet the transition from the trial to the inter-
387 trial interval was discontinuous, with population activity moving to an independent axis.
388 Our results thus show that the evolution of encoding of the present and of the past was
389 each along two independent axes.

390 Any neural population encoding both the past and the present in its activity faces
391 problems of interference: of how to prevent the addition of new information in the present
392 from overwriting the encoded information of the short-term past (Libby and Buschman,
393 2019); of how inputs to the population can selectively recall only the past or the present,
394 but not both; and of how downstream populations can access or distinguish the encodings
395 of the past and the present. Representing the present and past on independent axes solves
396 these problems. It means that the encoding of the present can be updated without altering
397 the encoding of the past, that inputs to the population can activate either the past or the
398 present representations independently, and that downstream populations can distinguish
399 the two by being tuned to read-out from one axis or the other. Indeed, we showed that
400 in post-session sleep the encoding of the present can be accessed independently of the
401 encoding of the past.

402 An open question is how much the clean independence between the encoding of the
403 past and present depends on the behavioural task. In the Y-maze task design, there is a
404 qualitative distinction between trials (with a forced choice) and inter-trial intervals (with
405 a self-paced return to the start arm), which we used to clearly distinguish encoding of the
406 present and the past. Such independent coding may be harder to uncover in tasks without
407 a distinct separation of decision and non-decision phases. For example, tasks where the
408 future choice of arm depends on recent history, such as double-ended T-mazes (Jones and
409 Wilson, 2005), multi-arm sequence mazes (Poucet et al., 1991), or delayed non-match to
410 place (Spellman et al., 2015), blur the separation of the present and the past. Comparing
411 population-level decoding of the past and present in such tasks would give useful insights
412 into when the two are, and are not, independently coded.

413 **Mechanisms for rapid switching of population codes**

414 The independent encoding and independent population activity between the trial and
415 immediately following inter-trial interval implies a rapid rotation of population activity.

416 How might such a rapid switch of network-wide activity be achieved?

417 Such rapid switching in the state of a network suggests a switch in the driver inputs
418 to the network. In this model, drive from one source input creates the network states for
419 population encoding A; a change of drive – from another source, or a qualitative change
420 from the same source – creates the network states for population encoding B (either set
421 of states may of course arise solely from internal dynamics). One option for a switching
422 drive is the hippocampal-prefrontal pathway.

423 Learning correlates with increased cortico-hippocampal coherence at the choice point
424 of this Y maze (Benchenane et al., 2010; Peyrache et al., 2009). This coherence recurred
425 during slow-wave ripples in post-training sleep. These data and our analyses here are
426 consistent with the population encoding of the trials being (partly) driven by hippocampal
427 input, and with the re-activation of only the trial representations in sleep being the
428 recruitment of those states by hippocampal input during slow-wave sleep. The increased
429 coherence between hippocampus and mPFC activity may act as a window for synaptic
430 plasticity of that pathway (Benchenane et al., 2010, 2011). Consistent with this, we saw a
431 correlation between performance improvement in trials and reactivation in sleep (see also
432 Maingret et al., 2016).

433 All of which suggests the encoding of the past during the inter-trial interval is not
434 driven by the hippocampal input to mPFC, as its representation is not re-activated in sleep.
435 (Spellman et al. 2015 report hippocampal input to mPFC is necessary for the maintenance
436 of a cue location; though, unlike in our task, actively maintaining the location of this cue
437 was necessary for a later direction decision). Rather, the population coding during the
438 inter-trial interval could reflect the internal dynamics of the mPFC circuit. Indeed, network
439 models of working memory in the prefrontal cortex focus on attractor states created by its
440 local network (Compte et al., 2000; Durstewitz et al., 2000; Miller et al., 2005; Wimmer
441 et al., 2014). If somewhere close to the truth, this account of rapid switching suggests
442 that the hippocampal input to mPFC drives population activity in the trial, and a change
443 or reduction in that input allows the mPFC local circuits to create a different internal
444 state during the inter-trial interval. A prediction of this account is that perturbation of
445 the hippocampal input to the mPFC could disrupt its encoding of the past and present in
446 different ways.

447 **Reconciling mPFC roles in memory and choice**

448 We propose that our combined results here and previously (Maggi et al., 2018) support
449 a dual-function model of mPFC population coding, where the independent coding of the
450 past and present respectively support on-line learning and consolidation. This model is
451 somewhat counter-intuitive: our data suggest the representation of the present in mPFC
452 is used for offline learning, whereas the representation of the past is used online to guide
453 behaviour.

454 Under this model, the role of memory encoding in the inter-trial interval is to guide
455 learning online: reward tags past features whose conjunction led to successful outcomes
456 (for example, the conjunction of turning left when the light is on in the left arm). While
457 population activity in the inter-trial interval reliably encodes features of the past through-
458 out training, we previously showed that synchrony of the population only consistently
459 occurs immediately before learning (Maggi et al., 2018). This suggests that the synchroni-
460 sation of mPFC representations of features predicting success is correlated with successful
461 rule-learning. Consistent with such past-encoding contributing to online learning, we show
462 here that the encoding in the inter-trial interval are not carried forward long-term into
463 sleep.

464 By contrast, we report here representations of the present in the trial are carried
465 forward and reactivated in sleep. Reactivation of waking activity during slow-wave sleep
466 has been repeatedly linked to the consolidation of memories (Stickgold, 2005; Tononi and
467 Cirelli, 2014; Sawangjit et al., 2018). Indeed, interrupting the re-activation of putative
468 waking activity in hippocampus impairs task learning (Girardeau et al., 2009). Thus,
469 under the dual-function model, we propose the reactivation in mPFC of mixed encodings
470 of the present may be consolidating the conjunction of present features and choice that is
471 going to be successful when re-used in future.

472 Further insight into these and other ideas here would come from stable recordings
473 of the same population across multiple sessions, to track how encoding of the past and
474 present evolves and is or is not reused. In particular, it would be insightful to establish if
475 re-activated trial representations in sleep reappear in subsequent sessions.

476 Acknowledgments

477 We thank Adrien Peyrache for the data, discussions, and comments on early drafts of
478 this manuscript, Hazem Toutounji and Martin O’Neill for comments on drafts, and the
479 Humphries’ lab past and present (Abhinav Singh, Javier Caballero, Mat Evans, Francois
480 Cinotti, Tomas Fiers) for discussion. This work was supported by the Medical Research
481 Council [grant numbers MR/J008648/1 and MR/P005659/1]. The original data collection
482 was supported by the EU Framework (FP6) “ICEA” grant.

483 Author Contributions

484 M.D.H and S.M. designed the analyses. S.M. analysed the data. M.D.H and S.M. wrote
485 the manuscript.

486 Declaration of Interest

487 The authors declare no conflicts of interest.

488 References

- 489 Aoi, M. C., Mante, V., and Pillow, J. W. (2020). Prefrontal cortex exhibits multidimen-
490 sional dynamic encoding during decision-making. *Nature neuroscience*, 23:1410–1420.
- 491 Averbeck, B. B., Sohn, J.-W., and Lee, D. (2006). Activity in prefrontal cortex during
492 dynamic selection of action sequences. *Nat Neurosci*, 9:276–282.
- 493 Baeg, E. H., Kim, Y. B., Huh, K., Mook-Jung, I., Kim, H. T., and Jung, M. W. (2003).
494 Dynamics of population code for working memory in the prefrontal cortex. *Neuron*,
495 40(1):177–188.
- 496 Benchenane, K., Peyrache, A., Khamassi, M., Tierney, P. L., Gioanni, Y., Battaglia, F. P.,
497 and Wiener, S. I. (2010). Coherent theta oscillations and reorganization of spike timing
498 in the hippocampal- prefrontal network upon learning. *Neuron*, 66(6):921–936.
- 499 Benchenane, K., Tiesinga, P. H., and Battaglia, F. P. (2011). Oscillations in the prefrontal
500 cortex: a gateway to memory and attention. *Curr Opin Neurobiol*, 21(3):475–485.

-
- 501 Cavanagh, S. E., Towers, J. P., Wallis, J. D., Hunt, L. T., and Kennerley, S. W. (2018).
502 Reconciling persistent and dynamic hypotheses of working memory coding in prefrontal
503 cortex. *Nature communications*, 9:3498.
- 504 Compte, A., Brunel, N., Goldman-Rakic, P. S., and Wang, X. J. (2000). Synaptic mecha-
505 nisms and network dynamics underlying spatial working memory in a cortical network
506 model. *Cereb Cortex*, 10:910–923.
- 507 Constantinidis, C., Funahashi, S., Lee, D., Murray, J. D., Qi, X.-L., Wang, M., and
508 Arnsten, A. F. T. (2018). Persistent spiking activity underlies working memory. *Journal*
509 *of neuroscience*, 38:7020–7028.
- 510 Durstewitz, D., Seamans, J. K., and Sejnowski, T. J. (2000). Neurocomputational models
511 of working memory. *Nature Neuroscience*, 3:1184–1191.
- 512 Durstewitz, D., Vittoz, N. M., Floresco, S. B., and Seamans, J. K. (2010). Abrupt transi-
513 tions between prefrontal neural ensemble states accompany behavioral transitions during
514 rule learning. *Neuron*, 66(3):438–448.
- 515 Euston, D. R., Gruber, A. J., and McNaughton, B. L. (2012). The role of medial prefrontal
516 cortex in memory and decision making. *Neuron*, 76(6):1057–1070.
- 517 Euston, D. R., Tatsuno, M., and McNaughton, B. L. (2007). Fast-forward playback of
518 recent memory sequences in prefrontal cortex during sleep. *Science*, 318(5853):1147–
519 1150.
- 520 Fujisawa, S., Amarasingham, A., Harrison, M. T., and Buzsáki, G. (2008). Behavior-
521 dependent short-term assembly dynamics in the medial prefrontal cortex. *Nat Neurosci*,
522 11(7):823–833.
- 523 Fusi, S., Miller, E. K., and Rigotti, M. (2016). Why neurons mix: high dimensionality for
524 higher cognition. *Curr Opin Neurobiol*, 37:66–74.
- 525 Girardeau, G., Benchenane, K., Wiener, S. I., Buzsáki, G., and Zugaro, M. B. (2009).
526 Selective suppression of hippocampal ripples impairs spatial memory. *Nature Neuro-*
527 *science*, 12:1222–1223.
- 528 Guise, K. G. and Shapiro, M. L. (2017). Medial prefrontal cortex reduces memory inter-
529 ference by modifying hippocampal encoding. *Neuron*, 94:183–192.e8.
- 530 Hanks, T. D., Kopec, C. D., Brunton, B. W., Duan, C. A., Erlich, J. C., and Brody, C. D.
531 (2015). Distinct relationships of parietal and prefrontal cortices to evidence accumula-
532 tion. *Nature*, 520:220–223.
- 533 Hastie, T., Tibshirani, R., and Friedman, J. (2009). *The Elements of Statistical Learning*.
534 Springer, Berlin.
- 535 Horst, N. K. and Laubach, M. (2012). Working with memory: evidence for a role for the
536 medial prefrontal cortex in performance monitoring during spatial delayed alternation.
537 *Journal of neurophysiology*, 108(12):3276–3288.
- 538 Ito, H. T., Zhang, S.-J., Witter, M. P., Moser, E. I., and Moser, M.-B. (2015). A prefrontal-
539 thalamo-hippocampal circuit for goal-directed spatial navigation. *Nature*, 522(7554):50.

- 540 Jones, M. W. and Wilson, M. A. (2005). Theta rhythms coordinate hippocampal-prefrontal
541 interactions in a spatial memory task. *PLoS Biol*, 3(12):e402.
- 542 Jung, M. W., Qin, Y., McNaughton, B. L., and Barnes, C. A. (1998). Firing characteristics
543 of deep layer neurons in prefrontal cortex in rats performing spatial working memory
544 tasks. *Cereb Cortex*, 8(5):437–450.
- 545 Karlsson, M. P., Tervo, D. G., and Karpova, A. Y. (2012). Network resets in medial
546 prefrontal cortex mark the onset of behavioral uncertainty. *Science*, 338(6103):135–139.
- 547 Laskowski, C. S., Williams, R. J., Martens, K. M., Gruber, A. J., Fisher, K. G., and
548 Euston, D. R. (2016). The role of the medial prefrontal cortex in updating reward value
549 and avoiding perseveration. *Behavioural Brain Research*, 306:52–63.
- 550 Laubach, M., Amarante, L. M., Swanson, K., and White, S. R. (2018). What, if anything,
551 is rodent prefrontal cortex? *eNeuro*, 5.
- 552 Laubach, M., Caetano, M. S., and Narayanan, N. S. (2015). Mistakes were made: neural
553 mechanisms for the adaptive control of action initiation by the medial prefrontal cortex.
554 *Journal of Physiology-Paris*, 109(1):104–117.
- 555 Libby, A. and Buschman, T. J. (2019). Rotational dynamics reduce interference between
556 sensory and memory representations. *bioRxiv*, page 641159.
- 557 Lundqvist, M., Herman, P., and Miller, E. K. (2018). Working memory: Delay activity,
558 yes! persistent activity? maybe not. *Journal of neuroscience*, 38:7013–7019.
- 559 Maggi, S., Peyrache, A., and Humphries, M. D. (2018). An ensemble code in medial pre-
560 frontal cortex links prior events to outcomes during learning. *Nature Communications*,
561 9.
- 562 Maingret, N., Girardeau, G., Todorova, R., Goutierre, M., and Zugaro, M. (2016).
563 Hippocampo-cortical coupling mediates memory consolidation during sleep. *Nature*
564 *Neuroscience*, 19:959–964.
- 565 Miller, P., Brody, C. D., Romo, R., and Wang, X.-J. (2005). A recurrent network model
566 of somatosensory parametric working memory in the prefrontal cortex. *Cereb Cortex*,
567 15:679–679.
- 568 Murray, J. D., Bernacchia, A., Roy, N. A., Constantinidis, C., Romo, R., and Wang, X.-
569 J. (2017). Stable population coding for working memory coexists with heterogeneous
570 neural dynamics in prefrontal cortex. *Proceedings of the National Academy of Sciences*
571 *of the United States of America*, 114:394–399.
- 572 Narayanan, N. S. and Laubach, M. (2008). Neuronal correlates of post-error slowing in
573 the rat dorsomedial prefrontal cortex. *J Neurophysiol*, 100:520–525.
- 574 Peyrache, A., Khamassi, M., Benchenane, K., Wiener, S. I., and Battaglia, F. P. (2009).
575 Replay of rule-learning related neural patterns in the prefrontal cortex during sleep.
576 *Nature Neuroscience*, 12:919–926.
- 577 Poucet, B., Lucchessi, H., and Thinus-Blanc, C. (1991). What information is used by rats
578 to update choices in the radial-arm maze? *Behav Processes*, 25:15–26.

- 579 Powell, N. J. and Redish, A. D. (2016). Representational changes of latent strategies in
580 rat medial prefrontal cortex precede changes in behaviour. *Nature Communications*, 7.
- 581 Rich, E. L. and Shapiro, M. (2009). Rat prefrontal cortical neurons selectively code
582 strategy switches. *Journal of Neuroscience*, 29(22):7208–7219.
- 583 Rich, E. L. and Shapiro, M. L. (2007). Prelimbic/infralimbic inactivation impairs mem-
584 ory for multiple task switches, but not flexible selection of familiar tasks. *J Neurosci*,
585 27(17):4747–4755.
- 586 Rigotti, M., Barak, O., Warden, M. R., Wang, X.-J., Daw, N. D., Miller, E. K., and Fusi,
587 S. (2013). The importance of mixed selectivity in complex cognitive tasks. *Nature*,
588 497(7451):585–590.
- 589 Russo, E., Ma, T., Spanagel, R., Durstewitz, D., Toutounji, H., and Köhr, G. (2020).
590 Coordinated prefrontal state transition leads extinction of reward-seeking behaviors.
591 *bioRxiv*.
- 592 Sawangjit, A., Oyanedel, C. N., Niethard, N., Salazar, C., Born, J., and Inostroza, M.
593 (2018). The hippocampus is crucial for forming non-hippocampal long-term memory
594 during sleep. *Nature*, 564(7734):109.
- 595 Siegel, M., Buschman, T. J., and Miller, E. K. (2015). Cortical information flow during
596 flexible sensorimotor decisions. *Science*, 348(6241):1352–1355.
- 597 Singh, A., Peyrache, A., and Humphries, M. D. (2019). Medial prefrontal cortex population
598 activity is plastic irrespective of learning. *Journal of Neuroscience*, pages 1370–17.
- 599 Spaak, E., Watanabe, K., Funahashi, S., and Stokes, M. G. (2017). Stable and dynamic
600 coding for working memory in primate prefrontal cortex. *The Journal of neuroscience*
601 : the official journal of the Society for Neuroscience, 37:6503–6516.
- 602 Spellman, T., Rigotti, M., Ahmari, S. E., Fusi, S., Gogos, J. A., and Gordon, J. A. (2015).
603 Hippocampal-prefrontal input supports spatial encoding in working memory. *Nature*,
604 522(7556):309–314.
- 605 Stickgold, R. (2005). Sleep-dependent memory consolidation. *Nature*, 437(7063):1272.
- 606 Sul, J. H., Kim, H., Huh, N., Lee, D., and Jung, M. W. (2010). Distinct roles of rodent
607 orbitofrontal and medial prefrontal cortex in decision making. *Neuron*, 66(3):449–460.
- 608 Tononi, G. and Cirelli, C. (2014). Sleep and the price of plasticity: from synaptic and
609 cellular homeostasis to memory consolidation and integration. *Neuron*, 81(1):12–34.
- 610 Wasmuht, D. F., Spaak, E., Buschman, T. J., Miller, E. K., and Stokes, M. G. (2018).
611 Intrinsic neuronal dynamics predict distinct functional roles during working memory.
612 *Nature communications*, 9:3499.
- 613 Wimmer, K., Nykamp, D. Q., Constantinidis, C., and Compte, A. (2014). Bump attractor
614 dynamics in prefrontal cortex explains behavioral precision in spatial working memory.
615 *Nature Neuroscience*, 17:431–439.
- 616 Young, J. J. and Shapiro, M. L. (2009). Double dissociation and hierarchical organization
617 of strategy switches and reversals in the rat pfc. *Behavioral Neuroscience*, 123:1028–
618 1035.

619 **Methods**

620 **Task description and electrophysiological data**

621 All the data in this study comes from previously published data (Peyrache et al., 2009).
622 The full details of training, spike-sorting and histology can be found in (Peyrache et al.,
623 2009). The experiments were carried out in accordance with institutional (CNRS Comité
624 Opérationnel pour l’Ethique dans les Sciences de la Vie) and international (US National
625 Institute of Health guidelines) standards and legal regulations (Certificate no. 7186, French
626 Ministère de l’Agriculture et de la Pêche) regarding the use and care of animals.

627 Four Long-Evans male rats were implanted with tetrodes in the medial wall of pre-
628 frontal cortex, covering the prelimbic and infralimbic regions, and trained on a Y-maze
629 task (Figure 1a). During each session, neural activity was recorded for 20-30 minutes of
630 sleep or rest epoch before the training phase, in which rats worked at the task for 20-40
631 minutes. After that, another 20-30 minutes of sleep or rest epoch recording followed. Dur-
632 ing the sleep epochs, intervals of slow-wave sleep were identified offline from the local field
633 potential (details in Peyrache et al., 2009; Benchenane et al., 2010).

634 The Y-maze had symmetrical arms, 85 cm long, 8 cm wide, and separated by 120
635 degrees, connected to a central circular platform (denoted as the choice point throughout).
636 Each rat worked at the task phase by self-initiating the trial, leaving the beginning of the
637 start arm. A trial finished when the rat reached the end of the chosen goal arm. If the
638 chosen arm was correct according to the current rule, the rat was rewarded with drops of
639 flavoured milk. As soon as the animal reached the end of the chosen arm an inter-trial
640 interval started and lasted until the rat completed its self-paced return to the beginning
641 of the start arm.

642 Each rat was exposed to the task completely naïve and had to learn the rule by trial-
643 and-error. The rules were presented in sequence: go to the right arm; go to the cued arm;
644 go to the left arm; go to the uncued arm. The light cues at the end of the two arms were
645 lit in a pseudo-random sequence across trials, regardless of the rule in place.

646 The recording sessions taken from the study of Peyrache and colleagues (Peyrache
647 et al., 2009) were 53 in total. Each of the four rats learnt at least two rules, and they
648 respectively contributed 14, 14, 11, and 14 sessions. The learning, rule change, and other
649 sessions for each rat were intermingled. We used 49 sessions for most of the analysis. One
650 session was omitted for missing position data, one for consistent choice of the right arm (in
651 a dark arm rule) preventing decoder analyses (see below), and one for missing spike data
652 in a few trials. An additional session was excluded for having only two neurons firing in all
653 trials. Tetrode recordings were spike-sorted within each recording session. In the sessions
654 we analysed here, the populations ranged in size from 4-25 units. Spikes were recorded
655 with a resolution of 0.1 ms. Simultaneous tracking of the rat’s position was recorded at
656 30 Hz.

657 **Behavioural analysis**

658 Each session was classified according to its behavioural features. The learning sessions
659 were identified according to the original study (Peyrache et al., 2009) as the ones with
660 three consecutive correct trials followed by a performance of at least 80% correct. The
661 first of the three correct trials was the learning trial. Only ten sessions satisfied this
662 criterion. We quantified this learning as a step-like change in performance by fitting a
663 robust regression line to the cumulative reward curve before and after the learning trial.
664 The slopes of the two lines gave us the rate of reward accumulation before (r_{before}) and

665 after (r_{after}) the learning trial.

666 Eight rule change sessions were characterised by 10 consecutive correct trials or eleven
667 correct out of twelve trials followed by a change in the rule. The first trial with the new
668 rule was identified as the rule change trial. The change in performance in these sessions
669 was quantified with the same method above, with a robust regression line was fitted to
670 the cumulative reward curve before and after the rule change trial.

671 For all remaining sessions that were not rule change or putative learning sessions, we
672 assessed any performance change by fitting the piece-wise linear regression model to each
673 trial in turn (allowing a minimum of 5 trials before and after each tested trial). We then
674 found the trial at which the increase in slope ($r_{after} - r_{before}$) was maximised, indicating the
675 point of steepest inflection in the cumulative reward curve. We found 22 further sessions,
676 labelled “minor-learning”, in which we could find a positive inflection in the cumulative
677 reward curve.

678 **Linear decoding of task features**

679 To predict which task feature was encoded in mPFC population activity we trained and
680 tested a range of linear decoders (Hastie et al., 2009; Maggi et al., 2018). In the main
681 text we report the results obtained using a logistic regression classifier, but for robustness
682 we also tested three other decoders – linear discriminant analysis, (linear) support vector
683 machines, and a nearest neighbours classifier – and found similar results. The full details
684 of the decoding analysis can be found in Maggi et al. (2018).

685 Briefly, for each session, using the N active neurons in that session we constructed a
686 N -length vector of their firing rates in each trial \mathbf{r} , resulting in the set of population firing
687 rate vectors $\{\mathbf{r}(1), \dots, \mathbf{r}(T)\}$ across the T trials. Each trial’s task information was binary
688 labelled for three features: outcome (labels: 0, 1), the chosen arm (labels: left, right) and
689 the position of the light cue (labels: left, right). We used leave-one-out cross-validation
690 to decode each feature, holding out the i th trial’s vector $\mathbf{r}(i)$, training the classifier on the
691 $N - 1$ remaining trial vectors, and then using the resulting weight vector to predict the
692 feature’s label for the held-out trial. We quantified the accuracy of the decoder as the
693 proportion of correctly predicted labels over all T held out trials. The same approach was
694 used for the inter-trial intervals, by constructing \mathbf{r} for the firing rates in each inter-trial
695 interval.

696 For decoding at different positions in the maze, we first linearised the maze in five
697 equally-sized sections then computed the firing rate vector of the core population of length
698 N for each position p , \mathbf{r}^P . For each trial $t = 1, \dots, T$ and each section of the maze
699 $p = 1, \dots, 5$, the set of population firing rate vectors $\{\mathbf{r}^P(1), \dots, \mathbf{r}^P(T)\}$ was used to train
700 the decoder.

701 For each rat and each session, the distribution of outcomes and arm choices depended
702 on the rats’ performance, which could differ from 50%. Therefore, we trained and cross-
703 validated the same classifier on the same data-sets, but shuffling the labels of the task
704 features. In this way we obtained the accuracy of detecting the right labels by chance.
705 We repeated the shuffling and fitting 50 times and we averaged the accuracy across the
706 50 repetitions.

707 **Testing for independent encoding**

708 To compare the decoding accuracy between trials and inter-trial intervals, we trained
709 again the classifier using the population firing rate vectors computed on the entire maze
710 $\{\mathbf{r}(1), \dots, \mathbf{r}(T)\}$. We then trained the classifier on all the trials. We saved the population

711 vector of weights and we tested the model, optimised to decode trial activity, on every
712 inter-trial interval to evaluate the accuracy in decoding retrospective inter-trial interval
713 labels. The same procedure was used to train the linear classifier on all the inter-trial
714 intervals to test its accuracy in decoding trials activity. The population vector of weight
715 was also saved for this model.

716 The angle, θ , between the population vector of trials', w_t , and inter-trial intervals', w_I ,
717 weights was computed as $\theta = \cos^{-1} \left(\frac{w_t \cdot w_I}{\|w_t\| \|w_I\|} \right)$.

718 We further evaluated the independence of trial and inter-trial interval population vec-
719 tors by quantifying their separability in a low dimensional space. We used principal com-
720 ponents analysis (PCA) to project the population vectors of a session onto a common set
721 of dimensions. To do so, we constructed the data matrix \mathbf{X} from the firing rate vectors of
722 the core population, by concatenating trials and inter-trial intervals in their temporal or-
723 der $\{\mathbf{r}_t(1), \mathbf{r}_I(1), \dots, \mathbf{r}_t(T), \mathbf{r}_I(T)\}^T$; the resulting matrix thus had dimensions of $2T$ rows
724 and N (neurons) columns. Applying PCA to \mathbf{X} , we projected the firing rate vectors on to
725 the top d principal axes (eigenvectors of $\mathbf{X}^T \mathbf{X}$) to create the top d principal components.
726 For each set of d components, we quantified the separation between the projected trial and
727 inter-trial interval population vectors using a linear classifier (Support Vector Machine,
728 SVM), and report the proportion of misclassified vectors. We repeated this for between
729 $d = 1$ and $d = 4$ axes for each session.

730 Reactivation of task-feature encoding in sleep

731 In order to quantify the reactivation of waking activity in pre- and post-session sleep, we
732 used the population firing rate vectors computed for the decoder $\{\mathbf{r}(1), \dots, \mathbf{r}(T)\}$. We
733 considered here the average population vector for each session, computed across all the
734 trials for each feature. For example, we quantified the average population firing rate
735 vector for all the right choice trials, and separately for all the left choice trials. We then
736 compare the ranked average population firing rate vector for each feature with the firing
737 rate vector of each 1 second time bin of slow-wave sleep pre- and post-session. We used
738 Spearman's correlation coefficient to compare them and to quantify the difference between
739 the distributions of each feature and the slow-wave sleep pre- and post-session. Spearman's
740 coefficient was chosen specifically to remove any effects of global rate variations across the
741 vectors within or between epochs.

742 In order to have a reactivation of activity in post-session sleep, we expected the dis-
743 tribution of Spearman correlation coefficient between a feature and pre-session slow-wave
744 sleep to be leftward shifted compare to the distribution of Spearman correlation coefficient
745 between the same feature and post-session slow-wave sleep. We quantified this shift by
746 measuring the difference in the medians ($M_{post} - M_{pre}$) between the two distributions
747 of correlation coefficients. If the difference was positive then we had a higher correla-
748 tion of the population firing vector with the post-session slow-wave sleep compared to the
749 pre-session slow-wave sleep. If negative, then the population firing rate vector was more
750 similar to the pre-session slow-wave sleep population vector. To then control for different
751 time scales of reactivation in sleep we repeated the same procedure changing the time bin
752 in the slow-wave sleep pre- and post-session. We used time bins from 100 ms to 10 sec
753 every 150 ms for trials and from 10 sec to 200 sec every 2 sec for inter-trial intervals.

754 Data Availability

755 The spike-train and behavioural data that support the findings of this study are available
756 in CRCNS.org (DOI: 10.6080/K0KH0KH5), originating from (Peyrache et al., 2009).

757 Code to reproduce the main results of the paper is available at: [URL to come]